Enhanced Electron Screening in d(d,p)t for Deuterated Metals

C. Rolfs for LUNA Collaboration

Institut für Physik mit Ionenstrahlen, Ruhr-Universität Bochum, Germany

The electron screening effect in the d(d,p)t reaction has been studied for deuterated metals, insulators, and semiconductors, i.e. 58 samples in total. As compared to measurements performed with a gaseous D_2 target, a large effect has been observed in most metals, while a small (gaseous) effect is found e.g. for the insulators, semiconductors and lanthanides. The periodic table provides the ordering of the observed small and large effects in the samples. An explanation of the large effects in metals is possibly provided by the classical plasma screening of Debye applied to the quasi-free metallic electrons. The data also provide information on the solubility of hydrogen in the samples.

§1. Introduction

It is well known that the cross section $\sigma(E)$ of a charged-particle-induced nuclear reaction is enhanced at low energies by the electron clouds surrounding the interacting nuclides, with an enhancement factor[1)]

$$f_{\rm lab}(E) = E(E+U_{\rm e})^{-1} \exp(-2\pi\eta(E+U_{\rm e})+2\pi\eta(E)), \quad \text{for } S(E+U_{\rm e}) \approx S(E), \ (1\cdot1)$$

where $\eta(E)$ is the Sommerfeld parameter, $S(E)$ the astrophysical S-factor, and $U_{\rm e}$ the screening potential energy.

The screening effect in d(d,p)t has been studied previously for 6 deuterated metals,[2),3)] where the resulting $S(E)$ data showed for 4 metals an exponential enhancement according to equation (2). However, the extracted $U_{\rm e}$ values were about one order of magnitude larger than the value found in a gas-target experiment: $U_{\rm e} = 25$ eV.[4)] Our study of deuterated Ta led to $U_{\rm e} = 340 \pm 14$ eV[5),6)] confirming the previous observation. Recently, we reported on preliminary results for several metals, insulators, and semiconductors.[6),7)] The present report completes these investigations superseding the preliminary results.

§2. Experimental procedures

The equipment, procedures and data analysis have been described elsewhere.[5)–7)] The deduced thin-target yield curve, $Y(E_{\rm d}, q)$, is related to the cross section $\sigma(E_{\rm eff})$ via

$$Y(E_{\rm d}, q) = \alpha\epsilon_{\rm eff}(E_{\rm d})^{-1}\sigma(E_{\rm eff}), \qquad (2\cdot1)$$

with the effective energy $E_{\rm eff}$ and the constant α, as measured using a radioactive source. The effective stopping power $\epsilon_{\rm eff}(E_{\rm d})$ for the deuterated M_xD target is given by the expression

$$\epsilon_{\rm eff}(E_{\rm d}) = \epsilon_{\rm D}(E_{\rm d}) + x\epsilon_{\rm M}(E_{\rm d}). \qquad (2\cdot2)$$

Rutherford-Backscattering-Spectrometry of the samples exhibited no detectable surface contamination except for Al which revealed an Al_2O_3 surface layer with a thick-

ness of about 150 monolayers. Since this thickness is larger than the energy step in our differentiation method,[5] the reported $U_e \leq 30$ eV value[6] corresponded to the case of an Al_2O_3 insulator and not to an Al metal (Table I). Since Al oxides rapidly in air, we cleaned the Al surface *in situ* by Kr sputtering at 15 keV (at the 100 kV accelerator) removing at least 100 monolayers. After this cleaning the experimental procedure[5] was carried out leading to $U_e = 520 \pm 50$ eV for the metal Al (Table I). This surface cleaning by Kr sputtering was carried out subsequently as a first step in the experimental procedures, for each new sample as well as for all of the previously studied samples,[6),7] where the target temperature was always $T = 20$ °C; in particular, the noble metals Cu, Ag, and Au exhibited — after this cleaning procedure — also a large enhancement effect.

The resulting cross section $\sigma(E_{\rm eff})$ is illustrated in Fig. 1 in form of the astrophysical $S(E)$ factor for the examples Cu, Nd, Hf and Pt. The absolute scale was obtained by normalisation to previous work[4] at $E_d = 30$ keV including the effects of electron screening where applicable. The normalisation led to a value for the stoichiometric ratio x given in Table I in form of the hydrogen solubility $1/x$.

In the analysis of the data (e.g. Fig. 1) we assumed a bare $S(E)$ factor (i.e. for bare interacting nuclides) linearly increasing with energy, $S_b(E) = 43 + 0.54E$ [keV b] (center-of-mass energy E in keV), as found previously.[4),5] Relative to this function, the data were fitted with the enhancement factor of equation : the resulting U_e values are summarized in Table I. In one experiment, we increased the target temperature to $T = 100$ °C using diffilen oil supplied by a cryo-circulator (JULABO FP90), whereby a thermoelement had been placed behind the target to measure T with a precision of 2 °C (including beam-heating effects). For deuterated Pt we find $U_e = 530 \pm 40$ eV (with $1/x = 0.06$) showing a decrease of U_e with increasing T (for $T = 20$ °C: $U_e = 670 \pm 50$ eV, $1/x = 0.06$; Table I).

In another experiment, we used a deuterated Pt target and a ^{3}He ion beam in combination with the reaction d(^{3}He,p)^{4}He to study the associated electron screening effect; here we have $S_b(E) = 6.7 + 0.0243E$ [MeV b], with center-of-mass energy E in keV. The result is $U_e = 680 \pm 60$ eV showing that high U_e values do not depend on the kind of ion species but are a feature of the deuterated metals.

§3. Discussion

A comparison of the U_e values with the periodic table indicates a common feature (Fig. 2): for each group of the periodic table, the corresponding U_e values are either low ("gaseous") as for groups 3 and 4 and the lanthanides, or high such as for the groups 2, 5 to 12, and 15. Group 14 is an apparent exception to this feature: the metals Sn and Pb have a high U_e value, while the semiconductors C, Si, and Ge have a low U_e value indicating that high U_e values are a feature of metals. A similar situation is found for group 13: B = insulator, Al and Tl = metals. The indication is supported further by the insulators BeO, Al_2O_3 and CaO_2. The deuterated metals of groups 3 and 4 and the lanthanides have a high hydrogen solubility, of the order of one, and thus represent also insulators; their observed solubilities are consistent with previous work.[8] For the metals with high U_e values, the solubilities are reported to

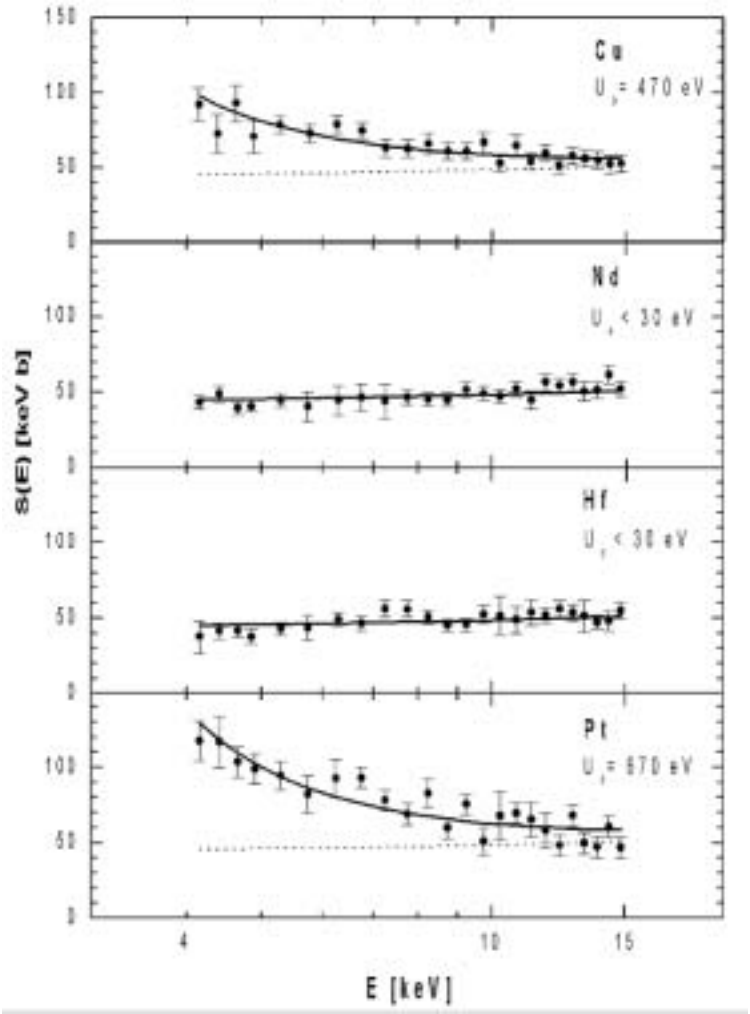

Fig. 1. Astrophysical $S(E)$ factor of the reaction d(d,p)t as obtained for the deuterated samples Cu, Nd, Hf and Pt (E = effective center-of-mass energy). The dotted curve represents the bare $S(E)$ factor, while the solid curve includes the exponential enhancement due to electron screening with the U_e value given.

be quite small, but actual values at room temperature are not available except for a few cases; the present work leads to solubilities of about 12% on average leaving the metallic character of the samples essentially unchanged.

Since the data for all metals with large U_e values could be fitted well with Eq. (1·1), the enhanced cross section is most likely due to electron effects of the environment of the target deuterons. Various aspects of the metals were discussed previously to explain possibly the data:[5),6)] stopping power, thermal motion, channeling, diffusion, conductivity, crystal structure, electron configuration, and "Fermi shuttle" acceleration mechanism; however, none of these aspects led to a solution.

If n_{eff} is the number of valence electrons per metallic atom which can be effec-

Table I. Summary of results.[a)]

	U_e (eV) [b)]	$1/x$ [c)]	n_{eff} [b)]	n_{eff}(Hall) [d)]
metals				
Be	180 ± 40	0.08	0.2 ± 0.1	(0.21 ± 0.04)
Mg	440 ± 40	0.11	3.0 ± 0.5	1.8 ± 0.4
Al	520 ± 50	0.26	3.0 ± 0.6	3.1 ± 0.6
V	480 ± 60	0.04	2.1 ± 0.5	(1.1 ± 0.2)
Cr	320 ± 70	0.15	0.8 ± 0.4	(0.20 ± 0.04)
Mn	390 ± 50	0.12	1.2 ± 0.3	(0.8 ± 0.2)
Fe	460 ± 60	0.06	1.7 ± 0.4	(3.0 ± 0.6)
Co	640 ± 70	0.14	3.1 ± 0.7	(1.7 ± 0.3)
Ni	380 ± 40	0.13	1.1 ± 0.2	1.1 ± 0.2
Cu	470 ± 50	0.09	1.8 ± 0.4	1.5 ± 0.3
Zn	480 ± 50	0.13	2.4 ± 0.5	(1.5 ± 0.3)
Sr	210 ± 30	0.27	1.7 ± 0.5	
Nb	470 ± 60	0.13	2.7 ± 0.7	(1.3 ± 0.3)
Mo	420 ± 50	0.12	1.9 ± 0.5	(0.8 ± 0.2)
Ru	215 ± 30	0.18	0.4 ± 0.1	(0.4 ± 0.1)
Rh	230 ± 40	0.09	0.5 ± 0.2	(1.7 ± 0.4)
Pd	800 ± 90	0.03	6.3 ± 1.3	1.1 ± 0.2
Ag	330 ± 40	0.14	1.3 ± 0.3	1.2 ± 0.3
Cd	360 ± 40	0.18	1.9 ± 0.4	(2.5 ± 0.5)
In	520 ± 50	0.02	4.8 ± 0.9	
Sn	130 ± 20	0.08	0.3 ± 0.1	
Sb	720 ± 70	0.13	11 ± 2	
Ba	490 ± 70	0.21	9.9 ± 2.9	
Ta	270 ± 30	0.13	0.9 ± 0.2	(1.1 ± 0.2)
W	250 ± 30	0.29	0.7 ± 0.2	(0.8 ± 0.2)
Re	230 ± 30	0.14	0.5 ± 0.1	(0.3 ± 0.1)
Ir	200 ± 40	0.23	0.4 ± 0.2	(2.2 ± 0.5)
Pt	670 ± 50	0.06	4.6 ± 0.7	3.9 ± 0.8
Au	280 ± 50	0.18	0.9 ± 0.3	1.5 ± 0.3
Tl	550 ± 90	0.01	5.8 ± 1.2	(7.4 ± 1.5)
Pb	480 ± 50	0.04	4.3 ± 0.9	
Bi	540 ± 60	0.12	6.9 ± 1.5	

	U_e (eV) [b)]	$1/x$ [c)]
semiconductors		
C	≤ 60	0.35
Si	≤ 60	0.23
Ge	≤ 80	0.56
insulators		
BeO	≤ 30	0.25
B	≤ 30	0.38
Al_2O3	≤ 30	0.27
CaO_2	≤ 50	0.60
groups 3 and 4		
Sc	≤ 30	1.4
Ti	≤ 30	1.3
Y	≤ 70	1.8
Zr	≤ 40	1.1
Lu	≤ 40	1.5
Hf	≤ 30	1.8
lanthanides		
La	≤ 60	0.6
Ce	≤ 30	1.3
Pr	≤ 70	0.9
Nd	≤ 30	0.7
Sm	≤ 30	1.3
Eu	≤ 50	0.6
Gd	≤ 50	1.4
Tb	≤ 30	1.3
Dy	≤ 30	1.1
Ho	≤ 70	1.6
Er	≤ 50	1.0
Tm	≤ 70	1.4
Yb	≤ 40	1.3

[a)] For a target temperature of $T = 20$ °C and a surface cleaning by Kr sputtering.
[b)] Error contains no systematic uncertainty in stopping power.
[c)] Estimated uncertainty is about 20%.
[d)] From the observed Hall coefficient at $T = 20$ °C, with an assumed 20% error; the numbers in brackets are for hole carriers.

tively treated as classical and quasi-free, one may apply the classical plasma theory of Debye leading to an electron sphere of radius[9)]

$$R_D = (\epsilon_0 kT/e^2 n_{eff}\rho_a)^{1/2} = 69(T/n_{eff}\rho_a)^{1/2} \quad [m] \tag{3·1}$$

around positive singly-charged ions (here: deuterons in the lattice) with the temperature of the free electrons T in units of K and the atomic density ra in units of m^{-3}. For $T = 293$ K, $\rho_a = 6 \times 10^{28}$ m^{-3}, and $n_{eff} = 1$ one obtains a radius

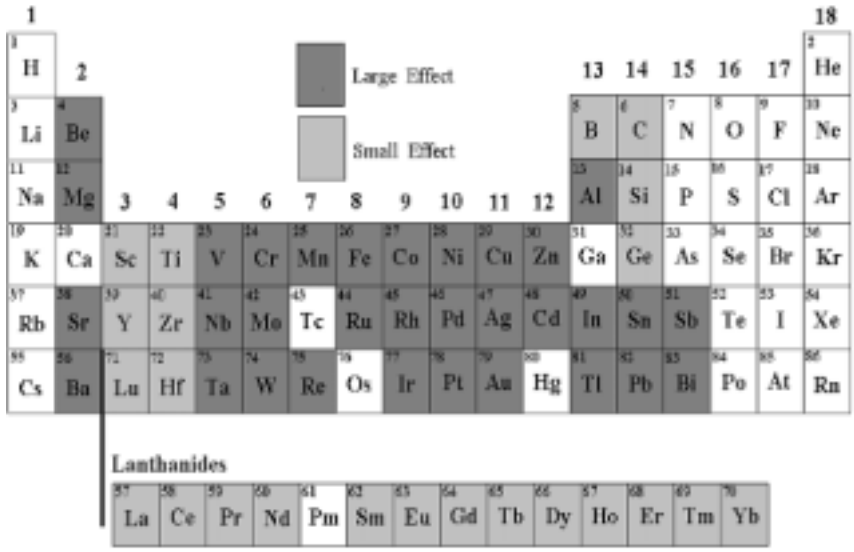

Fig. 2. Periodic table showing the studied elements, where those with low U_e values ($U_e < 100$ eV, small effect) are lightly shadowed and those with high U_e values ($U_e \geq 100$ eV, large effect) are heavily shadowed.

R_D, which is about a factor 10 smaller than the Bohr radius of a hydrogen atom. With the Coulomb energy between two deuterons at R_D set equal to U_e, one obtains $U_e = (4\pi\epsilon_0)^{-1}e^2/R_D = 300$ eV, the order of magnitude of the observed U_e values. A comparison of the calculated and observed U_e values leads to n_{eff} given in Table I: for most metals n_{eff} is of the order of one. The acceleration mechanisms of the incident ions leading to the high observed U_e values are thus — within our simple model — the Debye electron cloud at the rather small radius R_D.

A critical test of the classical Debye model is the predicted temperature dependence, $U_e \propto T^{-1/2}$. For deuterated Pt we find a ratio $R_{exp} = U_e(100\,^\circ\text{C})/U_e(20\,^\circ\text{C}) = 0.79 \pm 08$, in fair agreement with the expected value $R_{theo} = 0.88 \pm 0.01$ from our model. If one includes the observed $8 \pm 2\%$ decrease of n_{eff} over this temperature range (see below), the agreement is somewhat better ($R_{theo} = 0.84 \pm 0.02$). A new setup is in preparation to extend the measurements to significantly higher temperatures (more than 400 °C). It has been found that at low temperatures the hydrogen solubility increases rapidly such that the material becomes an insulator (e.g. Ta as reported in Ref. 5)).

An alternative determination of n_{eff} is obtained from the observed Hall coefficient for metals at room temperature (Ref. 10) and references therein),

$$C_{Hall} = (en_{eff}(\text{Hall})\rho_a)^{-1}, \tag{3·2}$$

where for about 50% of the metals in Table I the coefficient is negative (electron carriers) and for the other one-half it is positive (hole carriers). Since in the latter case essentially also electrons move (however in the opposite direction), we assumed that any dependence on the + or − sign of C_{Hall} can be neglected (which needs

theoretical verification). The resulting n_{eff}(Hall) values are also given in Table I: there is a remarkable correlation between n_{eff} and n_{eff}(Hall) both for electron and hole carriers, i.e. within 2 standard deviations the two quantities agree for all metals with a known Hall coefficient, except for Pd and Ir. Our own measurement of the Hall coefficient for Pd led to $n_{\mathrm{eff}}(\mathrm{Hall}) = 3.4 \pm 0.7$ removing essentially the discrepancy with $n_{\mathrm{eff}} = 6.3 \pm 1.3$. Thus, it appears desirable to measure or remeasure the Hall coefficient for all metals with a high U_{e} value (Table I).

Although the classical Debye model appears to explain to a large extent the data, it is well known that most of the conduction electrons are not classical but are frozen by quantum effects and only electrons close to the Fermi energy (E_{F}) actually should contribute to screening. A standard calculation of a Fermi gas at low temperature ($kT \ll E_{\mathrm{F}}$) yields an effective number $n_{\mathrm{eff}}(\mathrm{Fermi}) = 0.67kT/E_{\mathrm{F}}$ and correspondingly the screening potential energy U_{e} should be about 10 eV at room temperature (for $E_{\mathrm{F}} = 3$ eV). However, near room temperature the Hall coefficient C_{Hall} is observed for many metals to increase with temperature,[10] e.g. for Pt by 8% between $T = 20$ °C and 100 °C, while from n_{eff}(Fermi) one expects a decrease for C_{Hall} by 34% over this temperature range. Furthermore, inserting n_{eff}(Fermi) into Eq. (3·1), one expects no temperature dependence for U_{e}, in conflict with our observation. Thus, the data for the electron screening as well as for the Hall coefficient suggest some deviation from this simple however well established treatment of conduction electrons.

It should be pointed out finally that improved measurements of the electron screening effects in deuterated materials require an Ultra-High-Vacuum system with in situ analysis methods of high depth resolution such as SIMS, AES and XPS to characterize in deeper detail the environment of the deuterium atoms at the surface.

References

1) H. J. Assenbaum, K. Langanke and C. Rolfs, Z. Phys. A **327** (1987), 461.
2) K. Czerski et al., Europhys. Lett. **54** (2001), 449.
3) H. Yuki et al., JETP Lett. **68** (1998), 823.
4) Ue. Grife et al., Z. Phys. A **351** (1995), 107.
5) F. Raiola et al., Eur. Phys. J. A **13** (2002), 377.
6) F. Raiola et al., Phys. Lett. B **547** (2002), 193.
7) C. Bonomo et al., Nucl. Phys. A **719** (2003), 37c.
8) W. M. Mueller, J. P. Blackedge and G. G. Libowitz, *Metal Hydrides* (Academic Press, New York, 1968).
F. A. Lewis and A. Aladjem, *Hydrogen Metal Systems*, Solid State Phenomena, Vol. 49-50 (Scitec Publ., Zürich, 1996).
9) F. F. Chen, *Introduction to plasma physics and controlled fusion* (Plenum, New York, 1984).
10) Landolt-Börnstein, Vol. II. 6 (Springer, Berlin, 1959).
C. M. Hurd, *The Hall effect in metals and alloys* (Plenum Press, 1972).